Journal of Alloys and Compounds 509 (2011) 3166–3171

Contents lists available at ScienceDirect

Journal of Alloys and Compounds

journal homepage: www.elsevier.com/locate/jallcom

High temperature sublimation behavior of antimony in $CoSb_3$ thermoelectric material during thermal duration test

Degang Zhao[a,*], Changwen Tian[a], Yunteng Liu[a], Chengwei Zhan[a], Lidong Chen[b]

[a] Institute of New Materials, Shandong Academy of Sciences, 19 Keyuan Road, Jinan 250014, China
[b] Energy Materials Research Center, Shanghai Institute of Ceramics, Chinese Academy of Sciences, 1295 Dingxi Road, Shanghai 200050, China

ARTICLE INFO

Article history:
Received 12 August 2010
Received in revised form
24 November 2010
Accepted 25 November 2010
Available online 13 December 2010

Keywords:
Antimony
Thermoelectric
Sublimation
$CoSb_3$

ABSTRACT

The thermal duration test of $CoSb_3$ thermoelectric material was studied from 600 °C to 750 °C in vacuum. The present work showed that the sublimation of antimony in $CoSb_3$ material obeyed a parabolic law. Effective activation energy for the sublimation of antimony in $CoSb_3$ was estimated to be 44.5 kJ/mol. SEM results showed that the grain-boundary crack appeared in the initial period of test and the crack gradually evolved into the micro-void after thermal duration test. During the thermal duration period, the surface of $CoSb_3$ became degraded seriously and some bubbles of gasified antimony appeared on the samples. After thermal duration test of 16 days at 750 °C, thermoelectric performance of $CoSb_3$ declined obviously and *ZT* value decreased from 0.24 to 0.16 at 327 °C.

1. Introduction

Thermoelectric (TE) conversion, as a reliable and static heat-to-electricity conversion technique, has attracted worldwide attention for the applications in electronic cooling, waste heat recovery and special power generation [1–3]. The conversion efficiency and reliability of TE device are two major issues in device design. The conversion efficiency is greatly related with the figure-of-merit of TE materials and temperature difference. Therefore, once the TE material of device is selected, the reliability of TE material during serving time becomes an important issue.

Doped or filled $CoSb_3$-based skutterudite compounds have high *ZT* values and are regarded as one of the promising materials working at intermediate temperature region [4–7]. Lu et al. [8] synthesized the *p*-type $La_{0.5}Ce_{0.5}Fe_3CoSb_{12}$ with nanostructure via the route of hydro/solvo-hot press and *ZT* value reached 0.82 at 773 K. Li et al. [9] prepared the *n*-type $In_xCe_yCo_4Sb_{12}$ with nano-structured InSb phase by melt-quench-anneal-spark plasma sintering method and *ZT* of 1.43 was achieved at 800 K. Recently, Qiu et al. [10] synthesized the *p*-type $Ce_{0.2}Co_4Sb_{11.2}Sn_{0.8}$ and achieved high TE properties through scattering broad range of phonons with different frequencies. Therefore, $CoSb_3$-based thermoelectric generator is considered as one of the most suitable power generation system in many different industries. However, $CoSb_3$ material is vulnerable to be oxidized or sublimed in different working conditions and the oxidation products can increase the resistance and result in the degradation of TE properties. Furthermore, the sublimation products can diffuse or condense on the thermal insulation materials and the cold-side of the unicouples, which could result in the electrical short circuit. Therefore, it is essential to evaluate the reliability of $CoSb_3$-based materials under different serving circumstances. So far, few studies on the reliability evaluation of $CoSb_3$ material were reported. Hara [11,12] studied the surface oxidation of $CoSb_3$ and found that two layers of oxidation products were formed; nevertheless the kinetic analysis and oxidation mechanism of $CoSb_3$ material were not provided. Leszczynski et al. [13] evaluated the thermal stability of $CoSb_3$ in air and determined its starting temperature of oxidation. In our previous work, we investigated the oxidation behavior of $CoSb_3$ and discussed the related mechanism [14]. Accompanying the recent progress in the $CoSb_3$-based space power, it is necessary to evaluate the reliability of $CoSb_3$ working in vacuum.

In this study, we presented a detailed study on the sublimation behavior of Sb in $CoSb_3$ during thermal duration test in vacuum and reported some interesting results. As the $CoSb_3$-based space power generally works at about 500 °C, accelerated thermal duration tests (600–750 °C) were carried out in the research. Related sublimation behavior was attentively discussed. The results are beneficial to the technological use of TE generator.

* Corresponding author. Tel.: +86 531 88728308.
E-mail addresses: degangzhao@gmail.com, degang2008@163.com (D. Zhao).

0925-8388/$ – see front matter © 2010 Elsevier B.V. All rights reserved.
doi:10.1016/j.jallcom.2010.11.204

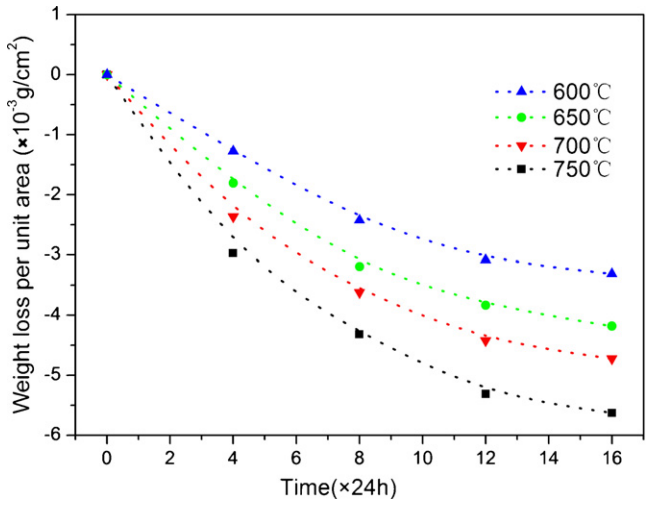

Fig. 1. Weight change per unit area of $CoSb_3$ material as a function of thermal duration time from 600 °C to 750 °C.

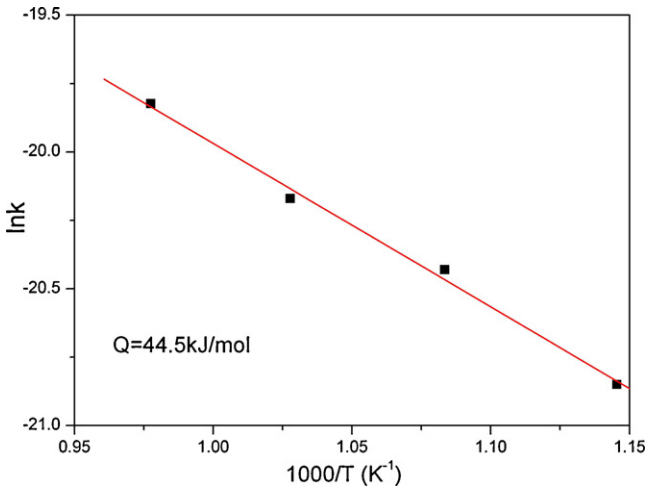

Fig. 2. Arrhenius plot of parabolic rate constant for sublimaton of Sb in $CoSb_3$ from 600 °C to 750 °C.

2. Experimental procedures

The $CoSb_3$ ingots were prepared by melting the starting materials in vacuum-encapsulated quartz tube at 1080 °C followed by annealing at 600 °C for 150 h. The resulting ingots were ground into powder and then sintered in a graphite die by spark plasma sintering (SPS) in vacuum at 590 °C under a pressure of 50 MPa for 600 s. The samples with the dimensions of $\varphi 10 \times 3$ mm were prepared from the sintered bulk $CoSb_3$. Both surfaces were metallographically polished down to 1 μm diamond paste and degreased in acetone before examination. Then the samples were sealed in quartz tubes and heated at a rate of 200 °C/h in the furnace to the testing temperature (600–750 °C). After keeping at the testing temperature for desired time (0–16 days), the samples were cooled to room temperature in furnace naturally. The mass changes were calculated by the difference after and before the thermal duration tests from an electronic balance with an accuracy of 0.1 mg. The surfaces of $CoSb_3$ samples were observed by scanning electron microscopy (SEM) and the chemical composition was investigated by electron probe micro-analysis (EPMA, JEOL, JXA-8100) with an energy dispersive spectroscopy (EDS) system. Disc-type specimens with the dimensions of 10 mm (diameter) and 1 mm (thickness) were prepared for thermal conductivity. Thermal conductivity was measured by a laser flash method (NETZSCH, LFA427) in vacuum. The Hall coefficient R_H was measured at room temperature with a constant magnetic field of 1*T*. The carrier concentration n was determined using $n = 1/R_H e$, where e is the elementary electron charge. Parallelepiped specimens of dimensions 1.5 mm × 1.5 mm × 8 mm cut from the disc-shaped sample were used for the measurements of Seebeck coefficient and electrical

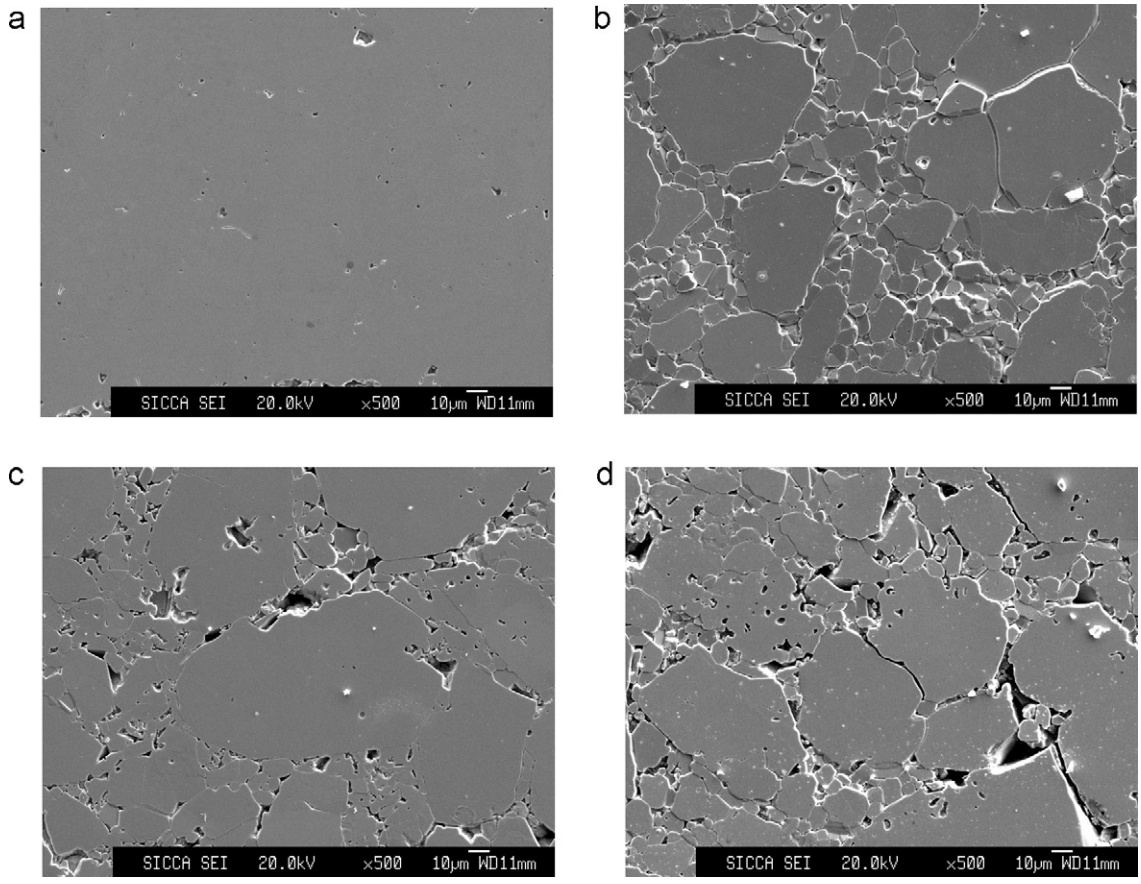

Fig. 3. Surface images of $CoSb_3$ after thermal duration test at 600 °C in vacuum for (a) 0 day, (b) 4 days, (c) 8 days, (d) 16 days.

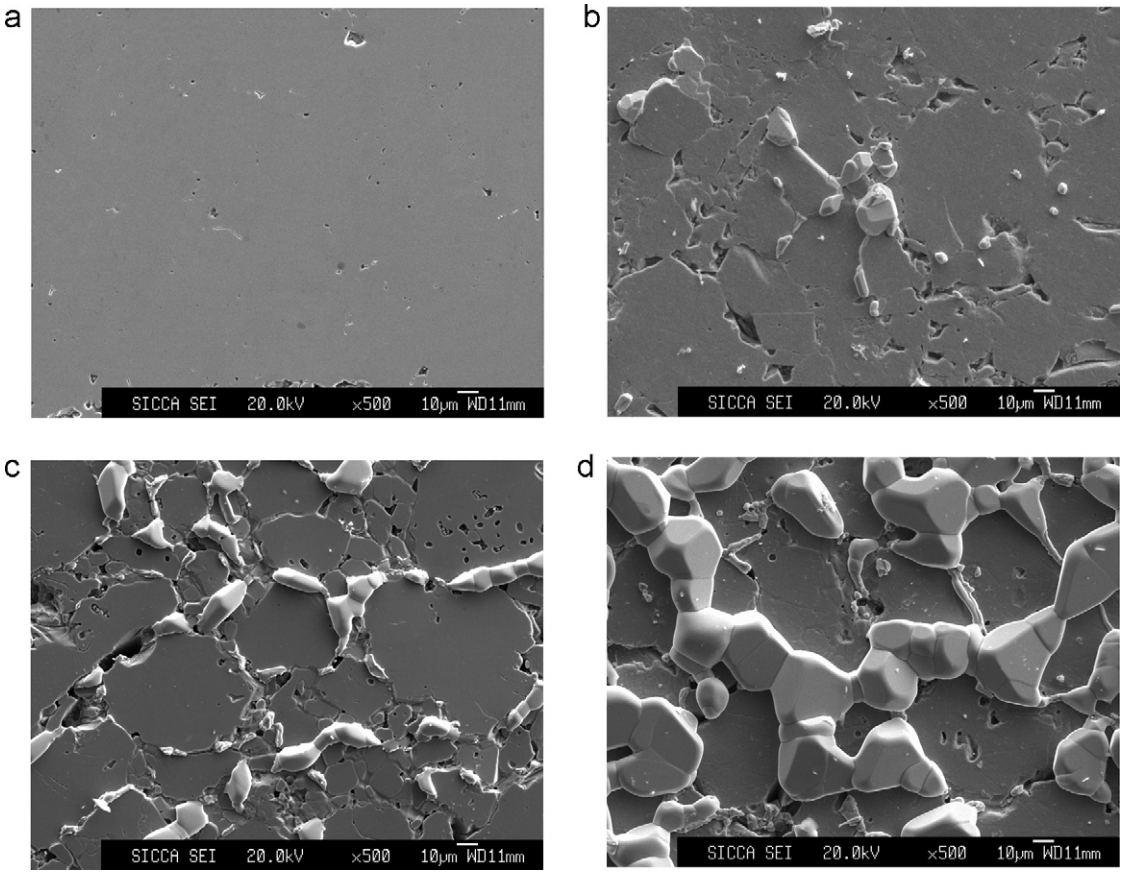

Fig. 4. Surface images of $CoSb_3$ after thermal duration test at 750 °C in vacuum for (a) 0 day, (b) 4 days, (c) 8 days, (d) 16 days.

conductivity, which were carried out by the standard four-probe method (ULVAC-RIKO, ZEM-2) in a flowing Ar atmosphere. All measurements were performed in a temperature range of 27–527 °C.

3. Results and discussion

3.1. Sublimation kinetics

Fig. 1 shows the weight change per unit area of $CoSb_3$ material as a function of thermal duration time in the temperature range from 600 °C to 750 °C in vacuum. It can be observed that the weight loss of $CoSb_3$ material from 600 °C to 750 °C was in excellent agreement with a parabolic rate law, which should be related with the sublimation of antimony. In addition, the sublimation of Sb was more intensive at higher temperature. Generally the weight loss of isothermal sublimation kinetics in the parabolic rule is expressed as by a rate equation:

$$(\Delta m)^2 = k_p \cdot t, \tag{1}$$

where Δm is the weight loss per unit area, k_p the rate constant and t is the time [15,16]. And k_p follows an Arrhenius relation of the type:

$$k_p = k_0 \exp\left(-\frac{Q_{\text{eff}}}{RT}\right), \tag{2}$$

where Q_{eff} could be reflected by the slope coefficient from the ln k_p versus $1/T$ plot during sublimation. After calculation, it was noted that the parabolic rate constant (k_p) increased from 8.7×10^{-12} g^2 cm^{-4} s^{-1} at 600 °C to 24.6×10^{-12} g^2 cm^{-4} s^{-1} at 750 °C, suggesting the sublimation of Sb was prone to occur at higher temperature. Effective activation energy for the sublimation of antimony in $CoSb_3$ was calculated to be 44.5 kJ/mol, as shown in Fig. 2. According to the definition of sublimation rate $k_s = \Delta m/t$, the sublimation rate calculated is 1.5×10^{-5} g/cm^2 h at 750 °C after thermal duration test of 16 days, which is lower than that of Yb-doped skutterudite under the same conditions [17]. The reason for high sublimation rate of the latter is probably due to the combined sublimation of Sb and Yb. The sublimation of antimony during thermal duration test demonstrates that the sublimation suppression for $CoSb_3$ material is essential for industrial application.

3.2. Morphology, phase composition and sublimation mechanism

The surface morphology and phase composition of $CoSb_3$ after thermal duration test were analyzed by SEM and EDS. Fig. 3 shows the surface images of $CoSb_3$ after thermal duration test at 600 °C in vacuum. It can be noted that grain-boundary crack appeared in the initial period of test and the crack gradually evolved into the micro-void after thermal duration test of 16 days. Similar results were also observed on the $CoSb_3$ samples after thermal duration test at 650 °C and 700 °C. Furthermore, after thermal duration test at 750 °C, some polyhedron crystallites were precipitated in the grain boundary and with the thermal duration time increasing, the polyhedron crystallites became coarser, just as shown in Fig. 4. With the help of EDS, the polyhedron crystallites were analyzed to be antimony, as shown in Figs. 5 and 6 presents the result of EPMA line profiles from point A to B of the $CoSb_3$ sample. It can be seen that the concentration of antimony of inner grain was lower than that of grain boundary, indicating the sublimation of antimony arose from the grain boundary. During the thermal duration test, the sublimation of antimony in $CoSb_3$ sample can be expressed as the following equation [18]:

$$CoSb_3 = CoSb_2 + Sb(g). \tag{3}$$

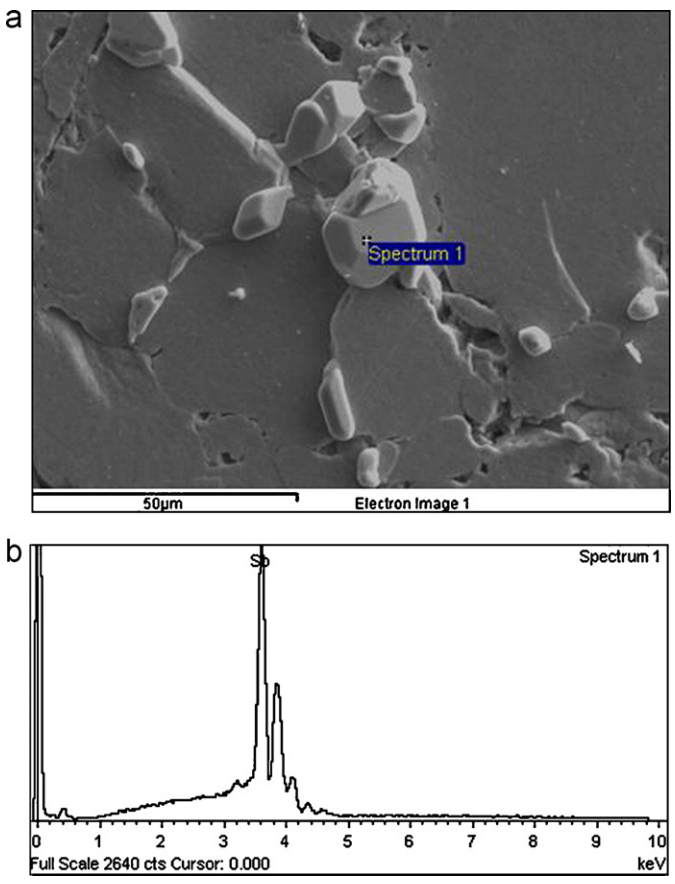

Fig. 5. (a) SEM of polyhedron crystallites, (b) EDS spectra.

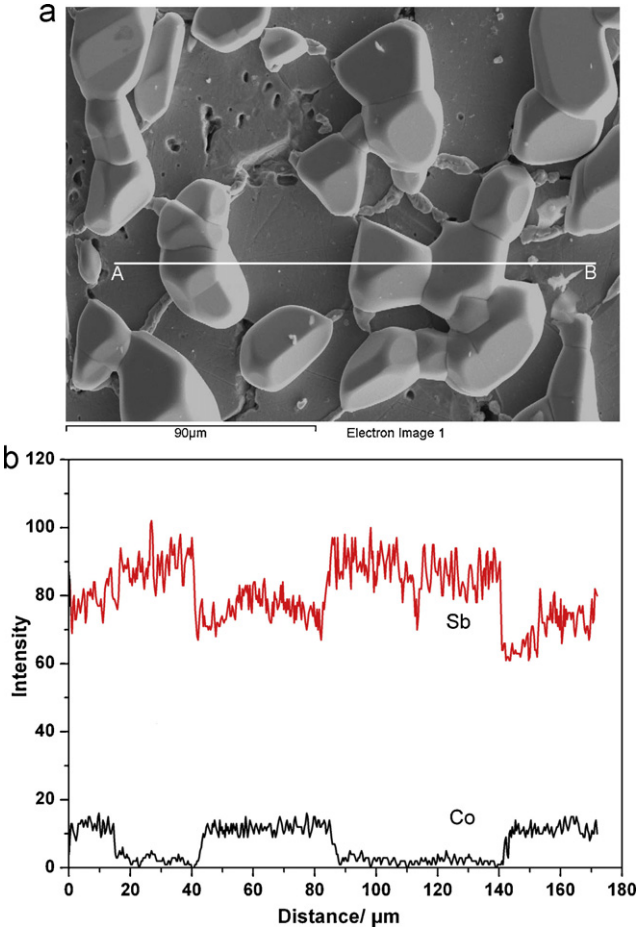

Fig. 6. (a) SEM image of antimony (b) EPMA line profiles from point A to B.

The gasified antimony gradually diffused into the grain boundary of $CoSb_3$ sample and then the sublimation phenomenon occurred. After thermal duration test of 16 days, the surface of $CoSb_3$ became degraded seriously and even appeared some bubbles of gasified antimony, just as shown in Fig. 7. The formation of bubble should be related with the pressure of gasified antimony. As the thickness of bubble is thin, it can be regarded as thin film. Assuming that the middle surface of bubble is a part of sphere, the pressure of gasified antimony can be expressed as:

$$p = nkT \tag{4}$$

where n is density of molecular number, k boltzmann constant and T is absolute temperature [19]. With the thermal duration time prolonging, n value increased and the bubble of gasified antimony grew gradually. According to the nonmomental theory, the stress of bubble is

$$\sigma = \frac{pR}{2t} = \frac{nkTR}{2t} \tag{5}$$

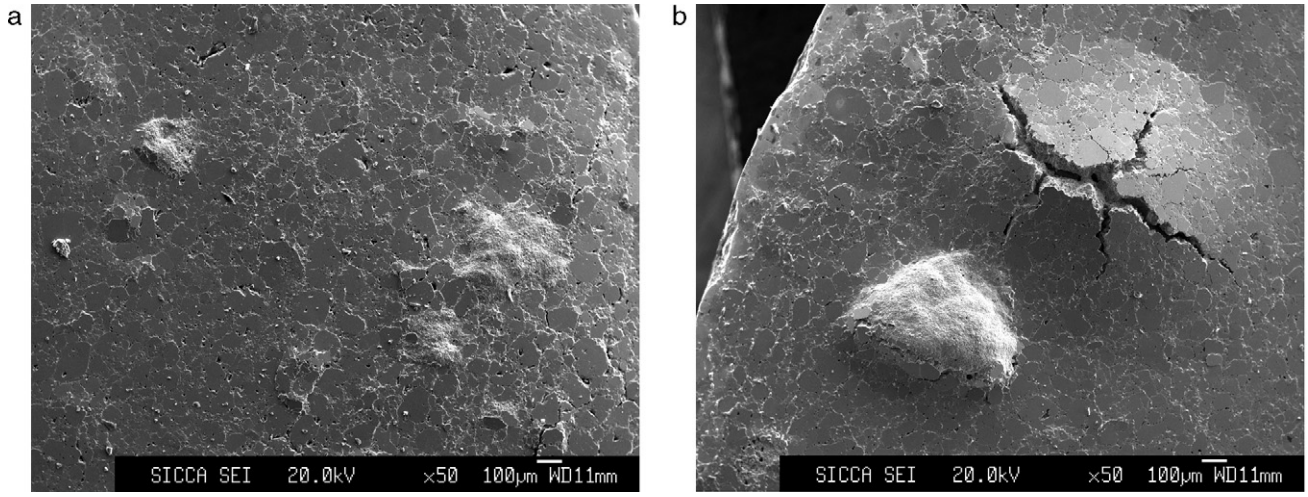

Fig. 7. Surface morphology of $CoSb_3$ material after thermal duration test in vacuum for 16 days at (a) 600 °C, (b) 750 °C.

where R is the radius of bubble and t is the time. It can be concluded that the surface tension depends closely on the sublimation rate of Sb. The sublimation of Sb was more intensive under higher temperature, resulting in the higher surface tension on the samples. When the surface of $CoSb_3$ samples cannot stand the stress resulting from the gasified antimony, the bubble of gasified antimony cracked.

3.3. Thermoelectric properties

As the sublimation of antimony changed the partial crystal structure and carrier concentration of $CoSb_3$ materials, the TE properties of $CoSb_3$ samples were definitely influenced. Fig. 8 is the XRD patterns of $CoSb_3$ after thermal duration test in vacuum for 16 days. It can be noted that the diffraction peak of $CoSb_2$ appeared after thermal duration test at 600 °C and 650 °C for 16 days; meanwhile, reflection from Sb was also observable after thermal duration test at 750 °C and 700 °C for 16 days, which was in accord with the SEM results above. The change of phase composition has an important influence on the TE properties of $CoSb_3$. Fig. 9 shows the TE properties of $CoSb_3$ material after thermal duration test in vacuum for 16 days. It can be seen that the electrical conductivity declined evidently after thermal duration test in vacuum at 750 °C for 16 days and the electrical conductivity at room temperature decreased by approximately 32%, as shown in Fig. 9(a). The decrease in electrical conductivity is considered to originate from the decline of carrier concentration due to the absence of Sb. The carrier concentration of un-tested $CoSb_3$ sample and tested sample (at 650 °C for 16 days) was 2.8×10^{19} cm^{-3} and 1.9×10^{19} cm^{-3}, respectively. After thermal duration test at 750 °C, the formation of micro-void suggested the $CoSb_3$ sample has high porosity, as shown in Fig. 4, which could leads to low electrical conductivity. On the other hand, the decline of electrical conductivity might be related with secondary phases such as $CoSb_2$ and Sb, which resulted from the phase transition (formula (3)) during the thermal duration test and has been detected in the XRD measurement. Klemens [20] has shown that the effect

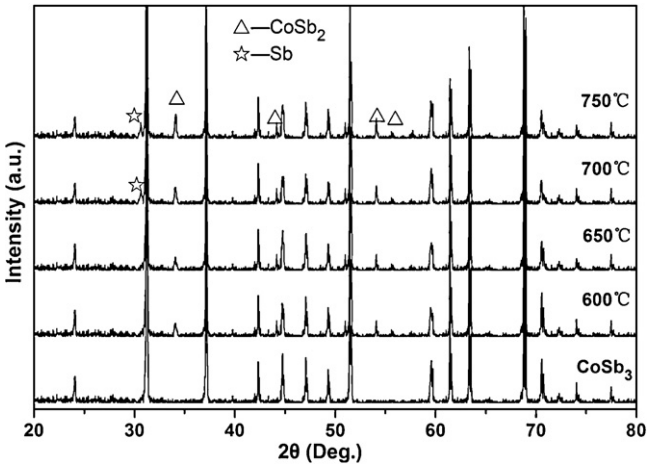

Fig. 8. X-ray diffraction patterns of $CoSb_3$ after thermal duration test in vacuum for 16 days.

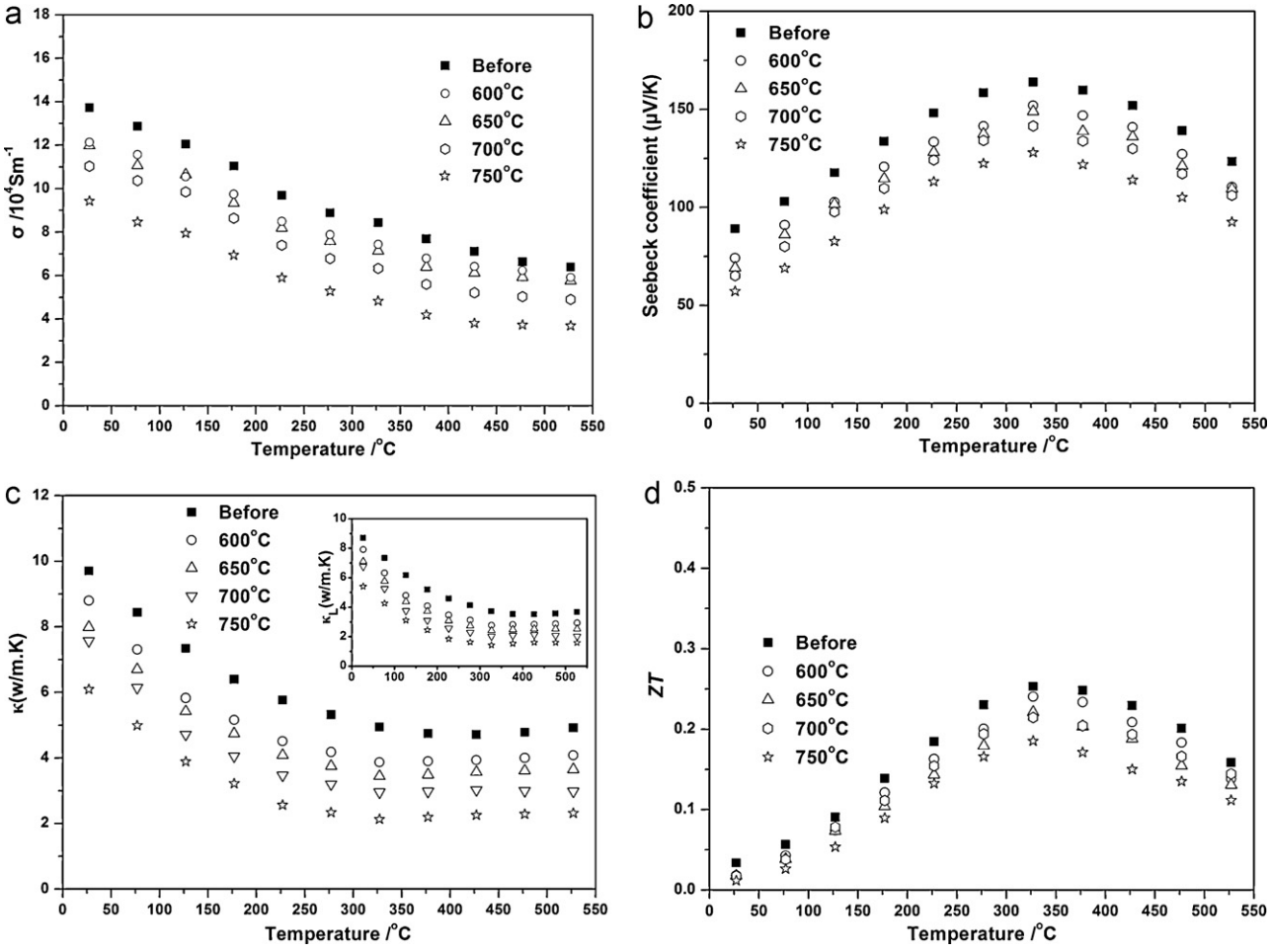

Fig. 9. Thermoelectric properties of $CoSb_3$ after thermal duration test in vacuum for 16 days; (a) electrical conductivity, (b) Seebeck coefficient, (c) thermal conductivity, (d) ZT.

Table 1
Thermoelectric properties of $CoSb_2$ [17] and $CoSb_3$ samples at room temperature.

Material	n (10^{19} cm^{-3})	σ (10^4 Sm^{-1})	α (μV K^{-1})	κ (Wm^{-1} K^{-1})
$CoSb_2$	1.5	11.2	35	11.7
$CoSb_3$	2.8	13.9	90	9.8

of second phase of material on the electrical conductivity is given by

$$\sigma_1 = \sigma_2 \left(1 + \frac{4f}{3}\right) \quad (6)$$

where σ_1 and σ_2 are the electrical conductivity of single- and two-phase material, respectively, and f is the volume fraction. Table 1 lists the comparison of TE properties of $CoSb_2$ and $CoSb_3$ samples [21]. The $CoSb_2$ phase was prone to form at 750 °C during thermal duration test, which could be reflected in XRD results of Fig. 8. Therefore, the electrical conductivity of $CoSb_3$ sample was lowest after the thermal duration test at 750 °C, just as shown in Fig. 9(a). Fig. 9(b) shows the Seebeck coefficient of $CoSb_3$ sample after thermal duration test. The $CoSb_3$ was still p-type conductivity after thermal duration test. The decrease in Seebeck coefficient is partially ascribed to the high porosity of $CoSb_3$ sample due to the sublimation of Sb. Another possible reason is the low Seebeck coefficient and electrical conductivity of $CoSb_2$ formed during the thermal duration test, which leads to a small decrease of the Seebeck coefficient of $CoSb_3$ samples. Similar results have been found in Hara's research [12].

Fig. 9(c) shows the thermal conductivity of $CoSb_3$ sample after thermal duration test. The thermal conductivity κ is the sum of the carrier thermal conductivity κ_c and the lattice thermal conductivity κ_L. The carrier thermal conductivity κ_c was estimated using the Wiedemann–Franz law,

$$\kappa_c = L\sigma T, \quad (7)$$

where L is the Lorenz number (2.45×10^{-8} V^2 K^{-2}) [22]. The lattice thermal conductivity κ_L was then obtained by subtracting the carrier contribution part from the overall thermal conductivity. After calculation, it can be concluded that the thermal conductivity of $CoSb_3$ was mainly attributed to the lattice contribution κ_L, as shown in Fig. 9(c). With the thermal duration time prolonging, the number of point defect or lattice defect increased due to the sublimation of Sb which enhanced the scattering of high-frequency phonon and decreased the mean free path of lattice phone. Therefore, the lattice conductivity decreased obviously after thermal duration test. The conversion efficiency of TE materials depends on the maximum ZT values. Fig. 9(d) indicates the change of ZT value of $CoSb_3$ materials after thermal duration test of 16 days. It can be seen that the ZT value of sample decreased significantly in the region of high temperature and the ZT value decreased from 0.24 to 0.16 at 327 °C after thermal duration test at 750 °C for 16 days. The sublimation of antimony in $CoSb_3$ put forward a new demand for the coating of $CoSb_3$-based skutterudites in the industrial application. The study about the coating for $CoSb_3$-based skutterudites will be carried out in future.

4. Conclusions

In this study, the thermal duration test in vacuum of $CoSb_3$ material was studied. The weight loss of $CoSb_3$ material from 600 °C to 750 °C was in excellent agreement with a parabolic rate law, which was related with the sublimation of antimony. The grain-boundary crack appeared in the initial period of test and the crack gradually evolved into the micro-void after thermal duration test. Polyhedron antimony crystallites were precipitated in the grain boundary during thermal duration test and with the thermal duration time increasing, antimony crystallites became coarser. After a certain thermal duration time, the surface of $CoSb_3$ became degraded seriously and some bubbles of gasified antimony appeared on the samples. After thermal duration test, TE properties of $CoSb_3$ were deteriorated and ZT value of $CoSb_3$ significantly decreased in high-temperature region.

Acknowledgements

This work is partly supported by Key Project for Transformation of Independent Innovation Achievements of Shandong Province in China granted no. 2009ZHZX1A0902 and Doctoral Fund of Shandong Academy of Sciences of China granted no. 2009022.

References

[1] R. Funahashi, M. Mikami, T. Mihare, S. Urata, N. Ando, J. Appl. Phys. 99 (2006) 066117.
[2] Y.P. Jiang, X.P. Jia, T.C. Su, N. Dong, F.R. Yu, Y.J. Tian, W. Guo, H.W. Xu, L. Deng, H.A. Ma, J. Alloys Compd. 493 (2010) 535.
[3] S.N. Zhang, T.J. Zhu, S.H. Yang, C. Yu, X.B. Zhao, J. Alloys Compd. 499 (2010) 215.
[4] S.Q. Bai, Y.Z. Pei, L.D. Chen, W.Q. Zhang, Acta Mater. 57 (2009) 3135.
[5] J.J. Zhang, B. Xu, F.R. Yu, D.L. Yu, Z.Y. Liu, J.L. He, Y.J. Tian, J. Alloys Compd. 503 (2010) 490.
[6] L. Zhang, N. Melnychenko-Koblyuk, E. Royanian, A. Grytsiv, P. Rogl, E. Bauer, J. Alloys Compd. 504 (2010) 53.
[7] Z. Xiong, X.H. Chen, X.Y. Huang, S.Q. Bai, L.D. Chen, Acta Mater. 58 (2010) 3995.
[8] P.X. Lu, F. Wu, H.L. Han, Q. Wang, Z.G. Shen, Xing Hu, J. Alloys Compd. 505 (2010) 255.
[9] H. Li, X.F. Tang, Q.J. Zhang, C. Uher, Appl. Phys. Lett. 94 (2009) 102114.
[10] P.F. Qiu, X. Shi, X.H. Chen, X.Y. Huang, R.H. Liu, L.D. Chen, J. Alloys Compd. 509 (2010) 1101.
[11] R. Hara, S. Inoue, H.T. Kaibe, S. Sano, in: Proc. 20th Inter. Conf. on Thermoelectrics, IEEE, Beijing, China, 2001, p. 84.
[12] R. Hara, S. Inoue, H.T. Kaibe, S. Sano, J. Alloys Compd. 349 (2003) 297.
[13] J. Leszczynski, A. Malecki, K. T. Wojciechowski, in: Proc. 5th Eur. Conf. on Thermoelectrics, IEEE, Odessa, Ukraine, 2007, p. 50.
[14] D.G. Zhao, C.W. Tian, S.Q. Tang, L.D. Chen, J. Alloys Compd. 504 (2010) 552.
[15] X.M. Wang, W.D. Wu, Y.J. Tang, X.Q. Zeng, S.S. Yao, J. Alloys Compd. 474 (2009) 499.
[16] X.K. Qian, Y.B. Li, Y. Sun, X.D. He, C.C. Zhu, J. Alloys Compd. 491 (2010) 386.
[17] T. Caillat, C.-K. Huang, B. Cheng, S.C. Chi, B. Li, E. Brandon, in: Proc. 7th Pacific Rim Conference on Ceramic and Glass Technology, Shanghai, China, 2007, p. 70.
[18] M. Chitroub, F. Besse, H. Scherrer, J. Alloys Compd. 467 (2009) 31.
[19] D. Chatterji, J.V. Smith, J. Electrochem. Soc. 120 (1973) 889.
[20] P.G. Klemens, Mater. Res. Soc. Symp. Proc. 234 (1991) 87.
[21] T.J. Caillat, Phys. Chem. Solids 57 (1996) 1351.
[22] Z. He, C. Stiewe, D. Platzek, G. Karpinski, E. Müller, J. Appl. Phys. 101 (2007) 053713.